The Water Energy Nexus: Improved Emergency Grid Restoration with DERs

Martin Pietsch and Florian Steinke
Energy Information Networks and Systems,
Technische Universität Darmstadt
Darmstadt, Germany
{martin.pietsch, florian.steinke}@eins.tu-darmstadt.de

***Abstract*—Water networks as critical infrastructures typically feature emergency electricity generators for bridging short power blackouts. We propose to combine these black start capable generators with available distributed energy resources (DERs) in the power grid, often photovoltaic generation, to jointly restore both the electricity and the water grid after blackouts. This is mutually beneficial for both networks since common grid-following inverters of DERs cannot supply power without a grid-forming nucleus. We model both grids as a coupled graph and formulate a stochastic mixed-integer linear program to determine optimal switch placement and/or switching sequences. Limited fuel and power availabilities, grid-forming constraints, storages, and an even distribution of available resources are considered. By minimizing the number of switching devices and switching events we target manual operability. The proposed method extends the time that can be bridged until a full restoration of the main power grid is achieved. For a small example, we demonstrate that given enough solar radiation our solution can double the water supply duration compared to using the generators only for the water network, while additionally resupplying almost half of the electricity demand. Algorithmic scaling is validated with a combination of the IEEE 123-bus test feeder and the D-Town water network.**

***Index Terms*—distribution grid restoration , network interdependencies, water-energy-nexus**

I. Introduction

Fresh water and electric power networks are both critical infrastructures with a major impact on human well-being in the case of crisis [1]. Since water pumps are dependent on electric power supply, water networks typically provide their own black start capable emergency power generators, i.e., diesel gensets, at the pump locations, to ensure service continuation in the case of blackouts. The fuel supply for these generators, however, mostly supports only limited blackout periods ($\sim$ 2 - 72 hours) [2], [3]. On the electric side, one can observe that more and more decentral energy resources (DERs) are available in today's grids, often based on renewable energy such as photovoltaic (PV) plants. While their energy supply is crisis-resistant, they are mostly operated in grid-following mode and thus cannot deliver their power to the grid in emergency situations without an operable (micro-) grid [4].

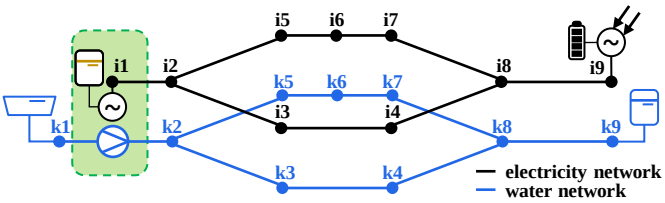

Fig. 1. Water and power networks are physically linked at pump sites (green box). Using the water grid's black start capable backup generator (i1) to build a micro-grid nucleus allows to integrate the grid-following photovoltaic plant (i9) and to partially re-supply electric demands in emergency situations, while extending the water supply duration through reduced fuel consumption from the genset's tank (yellow). Time-dependent switching sequences can use the flexibility from the water storage tank (k9), the water reservoir (k1), and the electric storage (i9).

We thus propose to combine the resources of both networks to their mutual benefit in long-lasting blackout situations, thereby improving overall disaster resilience. Available renewable energies can help reduce the fuel consumption of emergency generators in water networks and thereby extend emergency water supply duration. At the same time, the black-start capable, grid-forming emergency generators of the water system can serve as anchor points for building decentral electric islands that allow to connect available DER resources and, hence, to pick up some electric loads, see Figure 1 for an example.

Apart from supplying as many (critical) loads as possible we also target an even distribution of the limited energy resources. This is because a lack of power and water might not be critical for short periods, but supply interruptions over extended periods can rapidly reduce human well-being [5].

Our approach extends previous work on power grid restoration via emergency islands [6], suitably located emergency generators [7], [8] or power switches [9], and repair crew scheduling [10], [11]. The interdependence of critical infrastructures implies the possibility of correlated and cascading failures, see e.g. [12]–[16], and for water and electricity specifically [17]. Restoration schedules for interdependent networks can be determined based on network flow analysis [18] or

Submitted to the 22nd Power Systems Computation Conference (PSCC 2022). This work has been funded by the LOEWE initiative (Hesse, Germany) within the emergenCITY center.

the optimization of supply quality and resilience metrics, via a linear program [19], mixed-integer programs [20]–[22], or a mixed-integer second-order cone program [23]. While these approaches show the importance of cascading failures in interdependent networks and discuss their joint restoration, they do not address the mutual benefits that water grids' grid-forming emergency generators and power grids' available grid-following renewable sources together can offer. Moreover, even resource distribution among non-prioritized customers is so far not considered.

Our contribution is to propose mutually-beneficial restoration of the water and electricity grid with an even distribution of available resources among non-prioritized customers. To this end, we formulate a stochastic mixed-integer linear program (MILP) that can determine both optimal switching sequences for restoration and the optimal switching-device placement. Focusing on the switches, i.e., circuit breakers in the electric and valves in the water networks, means that we control the grid state via actuation options that are realistically available today. The number of switching operations and devices is minimized such that the resulting schedule can optimally be executed manually by support crews. This is important since most switches in the two networks are not remotely controllable today, especially not in blackout situations where communication is often limited [2].

We first demonstrate our approach for the simple network shown in Figure 1. We show how the emergency operation proceeds over the course of a typical day. The simulations proof increased supply quality in both infrastructures compared to restoring each grid individually. By integrating renewable generation that could not be used without the grid-forming capabilities of the water grid's generators the duration of full water supply can be doubled, while additionally supplying almost half of the electricity demands that would not be supplied otherwise. The scalability of our approach is demonstrated with a realistically-sized example, namely a combination of the IEEE 123-bus test feeder [24] and the D-Town water network [25].

In Section II we present our approach for determining emergency switching sequences as well as optimal switch placement. The experimental results are found in Section III. We conclude in Section IV.

II. Optimization Approach

The optimal emergency operation and/or the optimal placement of switches is determined through a MILP optimization problem. If only the operation schedules are desired, the optimization problem can be solved with fixed variables for the switch placement. If switch placement is to be optimized, we consider several scenarios for loads and renewable availability and optimize expected costs via the sample average approximation of stochastic programming [26]. We now describe the equations and the logic behind the different parts of the problem, consecutively covering the electricity and water network, their interconnections, and the objective function.

All parameters are denoted by capital or Greek letters and variables by lower case ones. Binary values are named u, other variables are real-valued. The operation schedule is computed for a set of time steps $\mathcal{T}$ with lengths ΔT_t. The total planning horizon is T and index t always denotes an element of $\mathcal{T}$ in this paper. To avoid an overload of indices we refrain from denoting scenario indices for all operation-dependent variables, except stated otherwise. Note that throughout the paper the word switch is supposed to mean both a circuit breaker in the electric grid as well as a valve in the water network.

A. Electric Grid

The electric grid is modeled as a set of vertices / buses $\mathcal{V}^E$ and edges / lines $\mathcal{E}^E$. We use the index i for electric buses and ij to denote electric edges from bus i to bus j. Ω_i^E denotes the electric neighbors of node i.

Potentially there could be a switch on each line and each node, separating the grid from the connected generators and loads. Generators and loads can actively exchange power with the grid, as indicated by $u_{i,t}^{a,E}$, only when the grid node has an acceptable voltage, $u_{i,t}^{b,E}$, and when the switch between the grid and the generator or load is closed, $u_{i,t}^{c,E}$. This condition can be expressed as

$$u_{i,t}^{a,E} \leq u_{i,t}^{c,E} \ , \ u_{i,t}^{a,E} \leq u_{i,t}^{b,E} \ , \ \forall i,t, \tag{1a}$$

$$u_{i,t}^{a,E} \geq u_{i,t}^{c,E} + u_{i,t}^{b,E} - 1 \ , \ \forall i,t. \tag{1b}$$

Closed line circuit breakers are denoted by $u_{ij,t}^{c,E}$.

Buses $\mathcal{G} \subseteq \mathcal{V}^E$ are the grid connection point of emergency generators, buses $\mathcal{R} \subseteq \mathcal{V}^E$ of renewables, and buses $\mathcal{B} \subseteq \mathcal{V}^E$ of battery energy storages. $p_{g,t}^{G2G}$ denotes the power delivered to the grid by generator $g \in \mathcal{G}$ at time $t \in \mathcal{T}$, $p_{r,t}^{Res}$ that of $r \in \mathcal{R}$, and $p_{b,t}^{B,out}$ and $p_{b,t}^{B,in}$ is the power exchange of $b \in \mathcal{B}$ to and from the grid. Let $p_{ij,t}$ denote the power flow on line $ij \in \mathcal{E}^E$ and $D_{i,t}^E$ the electric load of node i at time t. The nodal power balance then is

$$\sum_{g \in \mathcal{G}} p_{g,t}^{G2G} \delta_{i,g} + \sum_{r \in \mathcal{R}} p_{r,t}^{Res} \delta_{i,r} + \sum_{b \in \mathcal{B}} (p_{b,t}^{B,out} - p_{b,t}^{B,in}) \cdot \delta_{i,b} = \sum_{j \in \Omega_i^E} p_{ij,t} + D_{i,t}^E \cdot u_{i,t}^{a,E} \ , \forall i,t. \tag{2}$$

Here, the Kronecker δ is one iff its two arguments are identical. Note that this condition implies that loads can either be satisfied in full or have to be disconnected from the sources. We do not consider increased demand after an outage here. But this could be included with a few additional conditions [10]. All power injections are subject to constraints,

$$-\overline{P}_g^G \cdot u_{r,t}^{a,E} \leq p_{g,t}^{G2G} \leq \overline{P}_g^G \cdot u_{r,t}^{a,E} \ , \forall g,t, \tag{3a}$$

$$0 \leq p_{r,t}^{Res} \leq \overline{P}_{r,t}^{Res} \cdot u_{r,t}^{a,E} \ , \forall r,t, \tag{3b}$$

$$0 \leq p_{b,t}^{B,in} \leq \overline{P}_b^{B,in} \cdot u_{b,t}^{a,E} \ , \forall b,t, \tag{3c}$$

$$0 \leq p_{b,t}^{B,out} \leq \overline{P}_b^{B,out} \cdot u_{b,t}^{a,E} \ , \forall b,t, \tag{3d}$$

where $\overline{P}_g^G$, $\overline{P}_{r,t}^{Res}$, $\overline{P}_b^{B,in}$, $\overline{P}_b^{B,out}$ are the (possibly time-dependent) maximum power capacities of the corresponding components.

Renewable energies can feed their energy to the grid or use it to charge attached battery storage when no grid is available, denoted by $p_{b,t}^{Res,lc}$. Denoting the battery energy level as $e_{b,t}^B$ this can be described as

$$e_{b,t}^B = e_{b,t-1}^B + \Delta T_t((p_{b,t}^{B,in} + p_{b,t}^{Res,lc})\eta_{bat} - \frac{p_{b,t}^{B,out}}{\eta_{bat}}), \forall b, t, \tag{4a}$$

$$0 \leq e_{b,t}^B \leq \overline{E}_b^B \ , \forall b, t, \tag{4b}$$

$$0 \leq p_{b,t}^{Res,lc} \leq \overline{P}_{b,t}^{Res} \cdot (1 - u_{b,t}^{a,E}) \ , \forall b, t, \tag{4c}$$

with η_{bat} being the battery efficiency and $\overline{E}_b^B$ its storage capacity.

We use the common DC approximation to linearly model the power flow in terms of the phase angles $a_{i,t}$. If the electric network is meshed, this guarantees a plausible power distribution among the edges. For tree-like networks the equations do not yield any restrictions. Note that other linear power flow formulations like linear DistFlow [27] could be used equally well. If a line is disconnected, indicated by $u_{ij,t}^{c,E} = 0$, the power flow equation is balanced by a slack variable $s_{ij,t}^E$. We then have

$$p_{ij,t} = B_{ij}\left(a_{i,t} - a_{j,t}\right) + s_{ij,t}^E \ , \forall t, ij \ , \tag{5a}$$

$$-\overline{P}_{ij} \cdot u_{ij,t}^{c,E} \leq p_{ij,t} \leq \overline{P}_{ij} \cdot u_{ij,t}^{c,E} \ , \forall t, i, j \in \Omega_i^E, \tag{5b}$$

$$-M_p^E \cdot (1 - u_{ij,t}^{c,E}) \leq s_{ij,t}^E \leq M_p^E \cdot (1 - u_{ij,t}^{c,E}), \quad \forall t, ij, \tag{5c}$$

where B_{ij} is the susceptance of line ij, $\overline{P}_{ij}$ its transmission capacity, and M_p^E a big M value for the maximum possible phase angle difference over a line.

An important consideration when using inverter-interfaced renewables for emergency grid operations is that they cannot form a grid without a synchronous grid-forming generator in their island, at least not when they operate in grid-following mode as is the industry standard today. To ensure this condition,we introduce a virtual flow [28] that connects each node under voltage, $u_{i,t}^{b,E}$, to at least one grid-connected generator,

$$\sum_{g \in \mathcal{G}} f_{g,t}^E \delta_{i,g} - u_{i,t}^{b,E} = \sum_{j \in \Omega_i^E} (f_{ij,t}^E - f_{ji,t}^E) \ , \forall t, i, \tag{6a}$$

$$0 \leq f_{ij,t}^E \leq |\mathcal{V}^E| \cdot u_{ij,t}^{c,E} \ , \forall t, ij, \tag{6b}$$

$$0 \leq f_{g,t}^E \leq u_{g,t}^{c,E} \cdot |\mathcal{V}^E| \ , \forall g, t, \tag{6c}$$

Moreover, voltage-supply indicator $u_{i,t}^{b,E}$ should be active when a generator at the same location is grid-connected or when the other end of a connected line is voltage supplied,

$$u_{g,t}^{b,E} \geq u_{g,t}^{c,E} \ , \forall g, t, \tag{7a}$$

$$u_{i,t}^{b,E} \geq u_{j,t}^{b,E} + u_{ij,t}^{c,E} - 1 \ , \forall t, ij, \tag{7b}$$

$$u_{j,t}^{b,E} \geq u_{i,t}^{b,E} + u_{ij,t}^{c,E} - 1 \ , \forall t, ij. \tag{7c}$$

B. Water Network

Similarly to the electric grid, we model the water network as a set of vertices / nodes $\mathcal{V}^W$ and pipes / edges $\mathcal{E}^W$. We use the indices k for water nodes and kl to denote water pipes from node k to node l. Water loads and sources can exchange water with the grid, $u_{k,t}^{a,W}$, if the node has a sufficient head pressure, $u_{k,t}^{b,W}$, and the nodal valve to the water grid is open, $u_{k,t}^{c,W}$. This is ensured by the conditions

$$u_{k,t}^{a,W} \leq u_{k,t}^{c,W} \ , \ u_{k,t}^{a,W} \leq u_{k,t}^{b,W} \ , \ \forall k, t, \tag{8a}$$

$$u_{k,t}^{a,W} \geq u_{k,t}^{c,W} + u_{k,t}^{b,W} - 1 \ , \ \forall k, t. \tag{8b}$$

Open pipe valves are denoted by $u_{kl,t}^{c,W} = 1$.

The water network contains water reservoirs at nodes $\mathcal{C} \subseteq \mathcal{V}^W$ and water tanks at nodes $\mathcal{S} \subseteq \mathcal{V}^W$. The water flow from sources to the grid is denoted by $q_{c,t}^{Src}$ and from tanks $q_{s,t}^{Tank}$, respectively. The water demand of node k is $D_{k,t}^W$ and $q_{kl,t}$ is the water flow from k to l. The nodal water balance then is

$$\sum_{c \in \mathcal{C}} q_{c,t}^{Src} \delta_{k,c} - D_{k,t}^W u_{k,t}^{a,W} + \sum_{s \in \mathcal{S}} q_{s,t}^{Tank} \delta_{k,s} = \sum_{l \in \Omega_k^W} q_{kl,t}, \forall k, t, \tag{9}$$

where again a water load can only be supplied in full or not at all. The corresponding limits of the variables are

$$0 \leq q_{c,t}^{Src} \leq \overline{Q}_c^{Src} \cdot u_{c,t}^{c,W} \ , \forall c, t \tag{10a}$$

$$-u_{s,t}^{c,W} \overline{V}_s^{Tank} \leq q_{s,t}^{Tank} \Delta T_t \leq u_{s,t}^{c,W} \overline{V}_s^{Tank} \ , \forall s, t \tag{10b}$$

$$-M_q^W \cdot u_{kl,t}^{c,W} \leq q_{kl,t} \leq M_q^W \cdot u_{kl,t}^{c,W} \ , \forall t, kl \tag{10c}$$

where $\overline{Q}_c^{Src}$ is the maximum source flow, $\overline{V}_s^{Tank}$ the tank volume, and M_q^W the maximal possible water flow through a pipe. We thus assume that the tank can be filled or emptied within one time step, and further model the water storage via storage level $v_{s,t}^{Tank}$ as

$$v_{s,t}^{Tank} = v_{s,t-1}^{Tank} - q_{s,t}^{Tank} \Delta T_t \ , \forall s, t, \tag{11a}$$

$$0 \leq v_{s,t}^{Tank} \leq \overline{V}_s^{Tank} \ , \forall s, t. \tag{11b}$$

To describe the physics of the water flow, we use head pressures $h_{k,t}$ and follow a hydraulic model that considers pressure differences $h_{kl,t}^{\Delta H}$ due to topological height H_k and pressure losses that are linear in the mass flow through the pipes [29]. This is entailed by the following equations that hold for all pipe segments without pumps $\mathcal{P} \subseteq \mathcal{V}^W$,

$$h_{k,t} - h_{l,t} = h_{kl,t}^{\Delta H} + h_{kl,t}^{Loss} + s_{kl,t}^W \ , \forall t, kl \notin \mathcal{P}, \tag{12a}$$

$$h_{kl,t}^{\Delta H} = (H_k^H - H_l^H) \cdot u_{kl,t}^{c,W} \ , \forall t, kl, \tag{12b}$$

$$h_{kl,t}^{Loss} = K_{kl} q_{kl,t} \ , \forall t, kl, \tag{12c}$$

$$-M_h^W \cdot (1 - u_{kl,t}^{c,W}) \leq s_{kl,t}^W \leq M_h^W \cdot (1 - u_{kl,t}^{c,W}) \ , \forall t, kl, \tag{12d}$$

Here, $s_{kl,t}^W$ is a slack variable in case of a closed valve that renders the pressures at the two ends of a pipe independent. The pressure factor K_{kl} is given as $10.667 l_{kl} \lambda_{kl}^{-1.582} d_{kl}^{-4.871}$

where l_{kl} is the pipe length, d_{kl} its diameter, and λ_{kl} its surface roughness [30]. M_h^W is the maximum possible pressure difference over a pipe.

The sufficient head indicator $u_{k,t}^{b,W}$ is linked to the minimum head pressure $\underline{H}_{k,t}^{min}$ and as in (7) we ensure consistency,

$$h_{k,t} \geq \underline{H}_{k,t}^{min} \cdot u_{k,t}^{b,W} \ , \ \forall t, k, \tag{13a}$$

$$u_{k,t}^{b,W} \geq u_{l,t}^{b,W} + u_{kl,t}^{c,W} - 1 \ , \forall t, kl, \tag{13b}$$

$$u_{l,t}^{b,W} \geq u_{k,t}^{b,W} + u_{kl,t}^{c,W} - 1 \ , \forall t, kl. \tag{13c}$$

Concerning the pump characteristics, we limit the head pressure increase by the pump in terms of the flow with several linear segments described by parameters A_s and B_s with index s and we limit the minimum $\underline{Q}_{kl}^P$ and the maximum $\overline{Q}_{kl}^P$ flow,

$$h_{k,t} - h_{l,t} \leq q_{kl,t} \cdot A_s + B_s \ , \forall t, s, kl \in \mathcal{P}, \tag{14a}$$

$$\underline{Q}_{kl}^P \cdot u_{kl,t}^{c,W} \leq q_{kl,t} \leq \overline{Q}_{kl}^P \cdot u_{kl,t}^{c,W} \ , \forall t, kl \in \mathcal{P}. \tag{14b}$$

Unlike the electricity system, no virtual flow is needed here.

C. Interdependence

The electricity and the water network are interconnected through the power demand of the pumps. With $\gamma_{kl,g}$ indicating the connection of a pump on pipe $kl \in \mathcal{P}$ to generator $g \in \mathcal{G}$ we have

$$p_{g,t}^G = p_{g,t}^{G2G} + \sum_{kl \in \mathcal{P}} \gamma_{kl,g} q_{kl,t} \frac{\Delta H_{p,max}}{\eta_p} \ , \forall g, t \in \mathcal{P}, \tag{15a}$$

$$0 \leq p_{g,t}^G \leq \overline{P}_g^G \ , \forall g, t. \tag{15b}$$

Here, η_p is the efficiency of the pump and we have linearized its power consumption by assuming the maximum pressure rise in all cases. This slightly overestimates the required power and guarantees a conservative solution. This formulation also allows the generator to supply the pump directly without supplying the electric grid.

D. Switches and Switching

For the nodal switching indicators $u_{i/k,t}^{\rightleftharpoons,E/W}$ and the switch indicators $u_{i/k}^{s,E/W}$ we have

$$u_{i/k,t}^{\rightleftharpoons,E/W} \geq u_{i/k,t}^{c,E/W} - u_{i/k,t-1}^{c,E/W} \ , \forall i/k, t > 1, \tag{16a}$$

$$u_{i/k,t}^{\rightleftharpoons,E/W} \geq u_{i/k,t-1}^{c,E/W} - u_{i/k,t}^{c,E/W} \ , \forall i/k, t > 1, \tag{16b}$$

$$u_{i/k}^{s,E/W} \geq \frac{1}{|\mathcal{T}|} \sum_{t \in \mathcal{T}} u_{i/k,t}^{\rightleftharpoons,E/W}, \forall i/k, \tag{16c}$$

and similarly for the corresponding indicators on lines and pipes

$$u_{ij/kl,t}^{\rightleftharpoons,E/W} \geq u_{ij/kl,t}^{c,E/W} - u_{ij/kl,t-1}^{c,E/W} \ , \forall ij/kl, t > 1, \tag{17a}$$

$$u_{ij/kl,t}^{\rightleftharpoons,E/W} \geq u_{ij/kl,t-1}^{c,E/W} - u_{ij/kl,t}^{c,E/W} \ , \forall ij/kl, t > 1, \tag{17b}$$

$$u_{ij/kl}^{s,E/W} \geq \frac{1}{|\mathcal{T}|} \sum_{t \in \mathcal{T}} u_{ij/kl,t}^{\rightleftharpoons,E/W}, \forall ij/kl. \tag{17c}$$

Here, the notation E/W denotes that the conditions hold for both the electricity and the water network.

E. Objective Function

The target of our formulation is to minimize the number of switches x and the number of switching operations y. At the same time, we trade-off supply quality in both networks, as measured by the deficit costs z, versus fuel consumption.

The number of switching operations and switches is

$$x = \sum_t \left(\sum_{i/k} u_{i/k,t}^{\rightleftharpoons,E/W} + \sum_{ij/kl} u_{ij/kl,t}^{\rightleftharpoons,E/W}) \right), \tag{18a}$$

$$y = \sum_{i/k} u_{i/k}^{s,E/W} + \sum_{ij/kl} u_{ij/kl}^{s,E/W}. \tag{18b}$$

The deficit costs z penalize the average non-supplied time depending on each node's priority, expressed via weight $\Pi_{D,i/k}$, and prefer an even distribution of the individual non-supply durations $\overline{z}_{i/k}^{E/W}$, expressed by weight Π_D. Deviations of the individual non-supply duration from the average $\overline{z}^{E/W}$ are penalized quadratically. We use a discretization of the deviations with steps $d_w = |\mathcal{T}|w^2/(W-1)^2 - 10^{-8}$, $w = \{1, \dots, W\}$. With $u_{i/k,w}^z$ indicating the applicable deviation level we obtain

$$z = \sum_{i/k} \left(\frac{\Pi_{D,i/k}}{L^{E/W}} \overline{z}_{i/k}^{E/W} + \frac{\Pi_D D_{i/k}^{E/W}}{\overline{D}^{E/W}} \sum_w w^2 \, u_{i/k,w}^z \right), \tag{19a}$$

$$\overline{z}_{i/k}^{E/W} = T - \sum_t u_{i/k,t}^{a,E/W} \Delta T_t, \forall i/k, \tag{19b}$$

$$\overline{z}^{E/W} = \frac{1}{L^{E/W}} \sum_{i/k} \overline{z}_{i/k}^{E/W}, \forall i/k, \tag{19c}$$

$$-\sum_w u_{i/k,w}^z d_w \leq \overline{z}^{E/W} - \overline{z}_{i/k}^{E/W} \leq \sum_w u_{i/k,w}^z d_w, \forall i/k, \tag{19d}$$

$$\sum_w u_{i/k,w}^z \leq 1, \forall i/k. \tag{19e}$$

where $\overline{D}^{E/W}$ is the maximum demand and $L^{E/W}$ the number of demand nodes in each network, respectively.

The maximum allowed fuel consumption $\underline{L}_g^{fuel}$ is enforced as

$$\sum_t p_{g,t}^G \cdot \frac{\Delta T_t}{\eta_g \cdot H_{fuel}} \leq \underline{L}_g^{fuel} \ , \forall g, \tag{20}$$

where H_{fuel} is the caloric heating value of the fuel and η_g the generators' fuel efficiency.

The full optimization task then is the following stochastic program. Let σ denotes an element in the scenario set Σ and W_σ its probability. All variables are operation- and thus scenario-dependent except for the installation-dependent variables $u_{i/k}^{s,E/W}, u_{ij/kl}^{s,E/W}, y$. With weight parameters $\Pi_s^{\rightleftharpoons}$, Π_s, and Π_Δ we then aim to minimize the MILP

$$\begin{aligned} \min \ & \Pi_s^{\rightleftharpoons} \sum_\sigma W_\sigma x_\sigma + \Pi_s y + \Pi_\Delta \sum_\sigma W_\sigma z_\sigma, \\ \text{s.t.} \ & \forall \sigma \in \Sigma : \ (1) - (20). \end{aligned} \tag{21}$$

If we only target the operation optimization, the scenario set contains only a single scenario of interest and the installation-dependent variables are fixed.

III. Experimental Evaluation

We demonstrate our approach for two examples: individual switching actions, time-dependent supply and consumption patterns, and the behavior under cost parameter variations are examined for a small example with 9 nodes in the water and energy networks each. The computational applicability to larger examples is demonstrated for the IEEE 123-bus feeder [24] in combination with the D-Town water network [25]. The optimization problem was formulated using GAMS [31] and solved with CPLEX [32] to an optimality gap of 10%.

A. Small Case Study: 9-Node

The topology of the two networks is shown in Figure 1. The peak values of the electric and water loads are given in Table I together with the topological height of the water nodes. Each load varies proportionally over time as shown in Figure 2. The generator (i1) has a capacity of 50 kW, an efficiency of 40% and a fuel tank capacity of 214 liters. This corresponds to the fuel amount needed to supply the complete water demand with the generator for 24h. The PV plant (i9) has a capacity of 300kW and an availability profile depicted in Figure 2. The connected battery can store up to 100kWh with an efficiency of 90% both for charging and discharging. The pump is characterized by two linear pieces for the flow-pressure curve and its maximum head suffices to reach the highest point in the grid. The water tank (k9) has unlimited capacity. All parameters B_{ij} are set to $1500kW/rad$, water pipe parameters K_{kl} as $0.104m \cdot s/l$ throughout. The cost weights are $\Pi_s^{\rightleftharpoons} = \Pi_s = \Pi_{D,i/k} = \Pi_D = 1$ and $\Pi_\Delta = 10$. The model is instantiated for 24 hourly time steps. For the initial conditions, all switches and valves are set to allow for electricity or water flows, reflecting the conditions directly after the start of a blackout. The fuel tank is assumed to be full at time zero. Cyclic boundary conditions exist for the battery and the water tank. Note that we examine a scenario with an externally caused blackout here. When local disaster scenarios are considered, damaged components can be modeled via closed switches or reduced capacities.

TABLE I
Small interdependent network case studys node loads in both networks including height levels of the water network

i/k	$D^E_{i,max}$[kW]	$D^W_{k,max}$[l/s]	H^H_k[m]
2	20	5	10
3	40	4	20
4	60	6	30
5	20	8	40
6	70	9	45
7	10	1	50
8	30	1	55
9	20	0	60

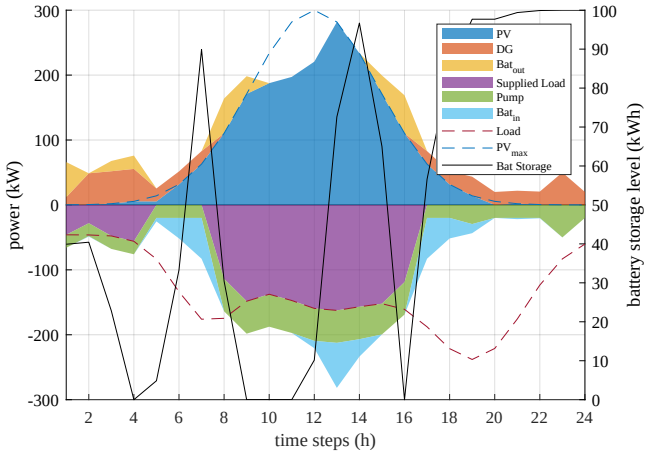

(a)

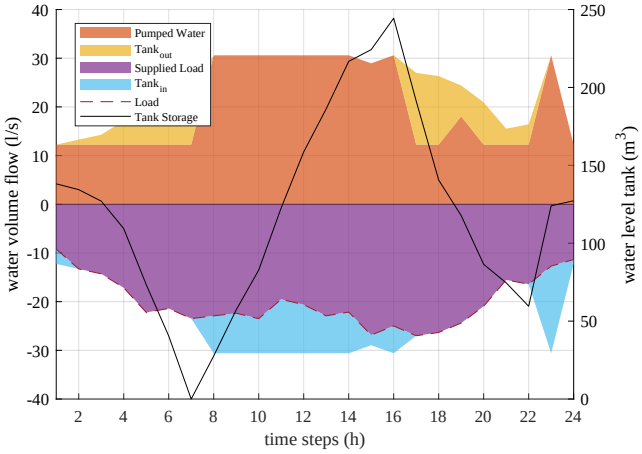

(b)

Fig. 2. Aggregated schedules for electricity (a) and for water (b) for one day of emergency operation of the 9-bus test network shown in Figure 1.

Figure 2 shows the computed operation schedules for $\underline{L}_g^{fuel} = 50\%$ of the tank volume, i.e. the computed emergency operation can be continued for two typical days. The simulation shows that we can supply all water demands and 50% of the electric demand while consuming only 50% of the fuel needed to supply the water alone. Note that the electric network could not be recovered if the water grid's emergency generators were not available as grid-forming anchors in the electric grid. This shows the great potential of using available renewable energy sources in emergency situations, to the benefit of both networks.

The operation schedule makes use of both the electric and the water storage, to maximally exploit the PV power when it is available. The available PV energy from time 9h to 15h cannot be fully utilized since the water pump is running at full capacity, while the battery is filled before the evening PV drop.

Figure 3 shows the supply status of the electric loads over the day, water loads are supplied throughout. The supply

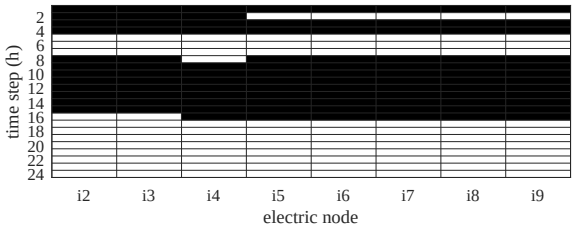

Fig. 3. The supply status (black is on) of the electric loads for the scenario shown in Figure 2.

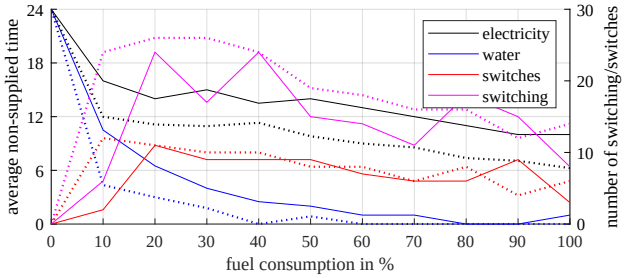

Fig. 4. Supply quality and number of switches for the 9-bus test example as a function of the fuel consumption $\underline{L}_g^{fuel}$, (solid) even distribution considered ($\Pi_D = 1$), (dashed) only average non-supply time minimized ($\Pi_D = 0$).

duration for all electric loads is identical, as targeted by our objective. Most electric supply is realized during the the same time periods. This can be explained both through the availability of solar energy during midday and the algorithm's target of minimizing the number of switches. It installs nodal switches in the electric grid at buses i2,i3,i4 and line switches at edges (i1,i2),(i2,i5),(i4,i8). The switch on line (i1,i2) allows to connect or disconnect all electric loads together, prioritizing pump supply as seen from 5am to 7am and 5pm to 12pm. The switches at line (i2,i5) and (i4,i8) allow to split the grid into two parts as seen in time step two, disconnecting the five loads of the upper-right part of the grid, while still being able to supply the lower-left part.

In Figure 4 we explore the optimization of switch placement in more detail. We show the trade-off between fuel consumption, average unsupplied time duration, and the number of switches and switching operations. For this experiment, we used two equally-probable scenarios to approximate the conditions during an unplanned outage. The first scenario is as described above whereas the second features a 30% reduction of the PV potential combined with an increase of the demands by 10%. Given the chosen weights in the objective, the water demands are supplied to a high degree except when only minimal fuel is available. The electric supply quality also increases with fuel availability, but more slowly. Since the generator does not have sufficient capacity to supply the electric loads at night time, unsupplied electric loads remain even when sufficient fuel is available. The more fuel can be used, the fewer switches and switching operations are needed to precisely control the loads. When allowing for uneven load supply, $\Pi_D = 0$, the supply quality can be increased.

In sum, the plot shows that without reducing the supply quality in the water network lots of electric loads can be supplied while at the same time fuel is saved as compared to a water-supply-only setup. The number of required switches and switching operations increases when less fuel can be used.

B. Large Case Study: IEEE 123 + D-Town

A larger test case is shown in Figure 5 where we combine the IEEE 123-bus test grid and the D-town water network, yielding a total of 531 nodes and 584 edges. We added 18 PVs of 500 kW peak power, two 2400 kWh battery storages as shown in Figure 5 and considered one scenario for PV availability. Electric loads are as given in the IEEE data set,

TABLE II
GENERATOR AND PUMP CHARACTERISTICS AT DIFFERENT LOCATIONS, SEE FIGURE 5.

Loc. name	node i	pump at kl	$\overline{P}_g^G$ [kW]
p1	3	372-368,371-367,370-369	500
p2	93	379-378,380-331	100
p3	59	375-4,376-377	100
p4	36	381-383,382-384	60
p5	101	385-387,386-388	80
-	40	-	500
-	73	-	130

summed up over all phases and assumed to be constant over time. For the water network, we take the topology and location of pumps, tanks, and reservoirs from the D-Town data set as well as the time-constant water loads. The pipe diameters were enlarged such that all loads can be supplied by the available pumps (the D-town test case is taken from a competition for optimizing water grid extensions). The pump's emergency generators are dimensioned to cover the pumps peak load and their fuel tanks are again sized to allow for one day of full water supply. Their specifications are given in Table II. The example also includes two generators without pumps. All switches initially allow for electricity or water flow, except the switches of the generators since these can not supply the whole electricity network in the first time step. The regions of the two networks were matched to each other as shown in Figure 5. We choose $\Pi_s^{\rightleftharpoons} = \Pi_s = \Pi_{D,i/k} = 1$, $\Pi_D = 0$, $\Pi_\Delta = 100$ and limit the fuel consumption to $\underline{L}_g^{fuel} = 50\%$. Moreover, we enforce full supply of the water network.

Our proposed approach allows to supply the electric loads 63.9% of the time on average, while each load except node (i76) is supplied at least 16.7% of the time. Node i76 has the highest demand that can not be supplied. The implementation of the proposed strategy requires 7 switches to be installed at the generators nodes, two switches at nodes with higher demand (i47,i76), and 10 line switches, see Figure 5. The switches are well-located to separate the grid into meaningful parts or to disconnect multiple loads at once (i65,i66).

The presented results use time steps of 4h-length, dividing the day into 6 discrete time steps. On a laptop, with an Intel i5-8265U CPU processor and 16 GB RAM, the computation

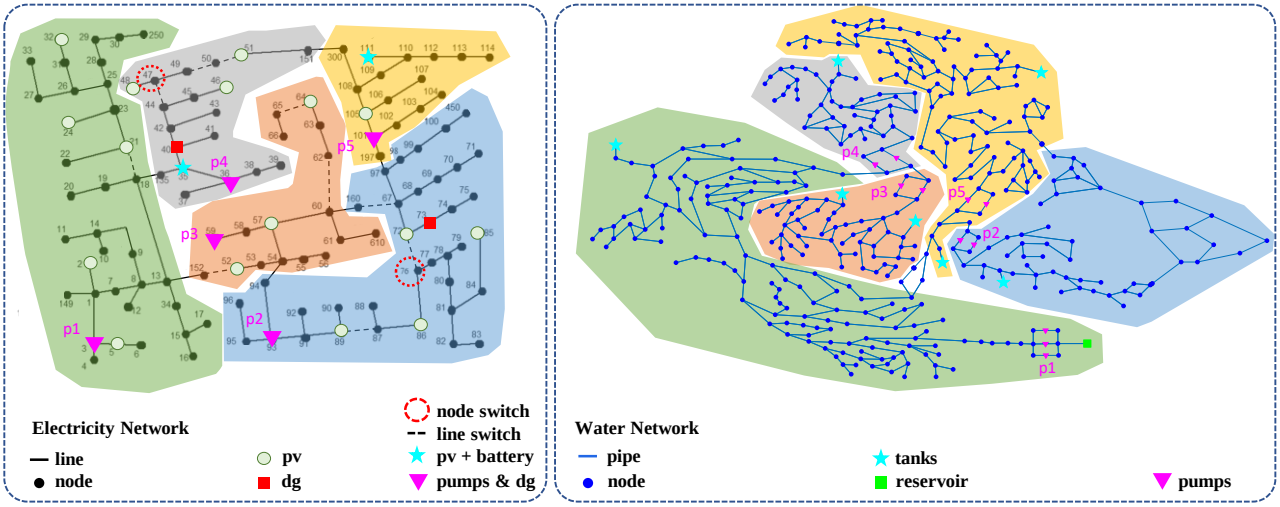

Fig. 5. Large test example combining the IEEE 123-bus grid with the D-Town network. The shading color denotes different water grid sections and their corresponding electric supply areas. Switches for an operating schedule that requires only 50% fuel are marked as dotted lines or red encircled.

time was 63 seconds. Due to the NP-hardness of the problem the computation times are strongly dependent on the choice of weights and the available fuel. A few minutes might be acceptable for longer emergency durations. Computation times could be improved by summarizing grid areas such that they can only be switched jointly and heuristics for parts of the problem could be developed.

IV. Conclusion

We present the first approach to transform the interdependence between the water and the energy network from a challenge into a source of opportunity. In order to do so, we formulated a stochastic mixed-integer linear program optimizing the operation of both networks in times of crisis. By minimizing the necessary number of switching devices we address the preparation stage, while optimizing switching events addresses the actual operation in times of crisis.

Without compromising (much) performance in the water network, water grid emergency generators can help to supply significant parts of the electricity grid by allowing for the integration of available, grid-following renewable generation in the electricity grid. Our approach can thus reduce the impact of blackouts on human well-being with small financial investments. If one spent large amounts of money on backup generators and fuel reserves, no times of under-supply would be necessary in both grids. However, given realistic, limited financial resources and rare emergency conditions, i.e., high impact low probability events, network resilience has to use whatever is available without much special-purpose hardware. We limit the investments to suitably located switches while accepting that some loads will not be supplied in full. This poses the ethically difficult question of whom to supply first or at all. We assumed that an even supply in terms of the supply duration, not the consumed energy, for non-critical loads would maximize social welfare.

Next steps will try to speed up the calculations, to stepwise discover the operational status of the components after an accident, to include communication constraints, and to implement the scheme in real-world applications.

References

[1] T. G. Lewis, *Critical infrastructure protection in homeland security: defending a networked nation*. John Wiley & Sons, 2019.

[2] T. Petermann, *Was bei einem Blackout geschieht: Folgen eines langandauernden und großflächigen Stromausfalls*, 2nd ed., ser. Studien des Büros für Technikfolgen-Abschätzung beim Deutschen Bundestag. Berlin: Edition sigma, 2013, vol. 33.

[3] J. Mayer, *Treibstoffversorgung bei Stromausfall: Empfehlung für Zivil- und Katastrophenschutzbehörden : Fachinformation*, ser. Praxis im Bevölkerungsschutz. Bonn: Bundesamt für Bevölkerungsschutz und Katastrophenhilfe, 2017, vol. 18.

[4] Paolone *et al.*, "Fundamentals of power systems modelling in the presence of converter-interfaced generation," *Electric Power Systems Research*, vol. 189, p. 106811, 2020.

[5] G. H. Haug, D. Spath, and H. Hatt, *The resilience of digitalised energy systems: Options of reducing blackout risks*. München and Halle (Saale) and Mainz: acatech - National Academy of Science and Engineering and German National Academy of Sciences Leopoldina and Union of the German Academies of Sciences and Humanities, 2021.

[6] B. Chen, C. Chen, J. Wang, and K. L. Butler-Purry, "Sequential service restoration for unbalanced distribution systems and microgrids," *IEEE Transactions on Power Systems*, vol. 33, no. 2, pp. 1507–1520, 2018.

[7] J. Shang, X. Sheng, J.-H. Zhang, and W. Zhao, "The optimized allocation of mobile emergency generator based on the loads importance," in *Asia-Pacific Power and Energy Engineering Conference*. Piscataway, NJ: IEEE, 2009, pp. 1–4.

[8] S. Lei, J. Wang, C. Chen, and Y. Hou, "Mobile emergency generator pre-positioning and real-time allocation for resilient response to natural disasters," *IEEE Transactions on Smart Grid*, p. 1, 2016.

[9] M. Gholami, J. Moshtagh, and N. Ghadernejad, "Service restoration in distribution networks using combination of two heuristic methods considering load shedding," *Journal of Modern Power Systems and Clean Energy*, vol. 3, no. 4, pp. 556–564, 2015.

[10] A. Arif, Z. Wang, C. Chen, and J. Wang, "Repair and resource scheduling in unbalanced distribution systems using neighborhood search," *IEEE Transactions on Smart Grid*, p. 1, 2019.

[11] N. Morshedlou, K. Barker, A. D. González, and A. Ermagun, "A heuristic approach to an interdependent restoration planning and crew routing problem," *Computers & Industrial Engineering*, vol. 161, p. 107626, 2021.

[12] L. Dueñas-Osorio, J. I. Craig, and B. J. Goodno, "Seismic response of critical interdependent networks," *Earthquake engineering & structural dynamics*, vol. 36, no. 2, pp. 285–306, 2007.

[13] S. V. Buldyrev, R. Parshani, G. Paul, H. E. Stanley, and S. Havlin, "Catastrophic cascade of failures in interdependent networks," *Nature*, vol. 464, no. 7291, pp. 1025–1028, 2010.

[14] M. Ouyang, "Review on modeling and simulation of interdependent critical infrastructure systems," *Reliability engineering & System safety*, vol. 121, pp. 43–60, 2014.

[15] S. Hasan and G. Foliente, "Modeling infrastructure system interdependencies and socioeconomic impacts of failure in extreme events: emerging R&D challenges," *Natural Hazards*, vol. 78, no. 3, pp. 2143–2168, 2015.

[16] H. Haes Alhelou, M. Hamedani-Golshan, T. Njenda, and P. Siano, "A survey on power system blackout and cascading events: Research motivations and challenges," *Energies*, vol. 12, no. 4, p. 682, 2019.

[17] E. Pournaras, R. Taormina, M. Thapa, S. Galelli, V. Palleti, and R. Kooij, "Cascading failures in interconnected power-to-water networks," *ACM SIGMETRICS Performance Evaluation Review*, vol. 47, no. 4, pp. 16–20, 2020.

[18] E. E. Lee II, J. E. Mitchell, and W. A. Wallace, "Restoration of services in interdependent infrastructure systems: A network flows approach," *IEEE Transactions on Systems, Man and Cybernetics, Part C (Applications and Reviews)*, vol. 37, no. 6, pp. 1303–1317, 2007.

[19] R. Holden, D. V. Val, R. Burkhard, and S. Nodwell, "A network flow model for interdependent infrastructures at the local scale," *Safety Science*, vol. 53, pp. 51–60, 2013.

[20] A. D. González, L. Dueñas-Osorio, M. Sánchez-Silva, and A. L. Medaglia, "The interdependent network design problem for optimal infrastructure system restoration," *Computer-Aided Civil and Infrastructure Engineering*, vol. 31, no. 5, pp. 334–350, 2016.

[21] Y. Almoghathawi, K. Barker, and L. A. Albert, "Resilience-driven restoration model for interdependent infrastructure networks," *Reliability Engineering & System Safety*, vol. 185, pp. 12–23, 2019.

[22] D. B. Karakoc, Y. Almoghathawi, K. Barker, A. D. González, and S. Mohebbi, "Community resilience-driven restoration model for interdependent infrastructure networks," *International Journal of Disaster Risk Reduction*, vol. 38, p. 101228, 2019.

[23] J. Li, Y. Xu, Y. Wang, M. Li, J. He, C.-C. Liu, and K. P. Schneider, "Resilience-motivated distribution system restoration considering electricity-water-gas interdependency," *IEEE Transactions on Smart Grid*, vol. 12, no. 6, pp. 4799–4812, 2021.

[24] IEEE PES Power System Analysis, Computing, and Economics Committee, "IEEE 123 Node test feeder," 2014. [Online]. Available: http://site.ieee.org/pes-testfeeders/files/2017/08/feeder123.zip

[25] Marchi *et al.*, "Battle of the water networks II," *Journal of Water Resources Planning and Management*, vol. 140, no. 7, 2014.

[26] A. Shapiro, *Stochastic programming by Monte Carlo simulation methods*. Humboldt-Universität zu Berlin, Mathematisch-Naturwissenschaftliche Fakultät II, Institut für Mathematik, 2000.

[27] M. E. Baran and F. F. Wu, "Optimal capacitor placement on radial distribution systems," *IEEE Transactions on power Delivery*, vol. 4, no. 1, pp. 725–734, 1989.

[28] T. Ding, K. Sun, C. Huang, Z. Bie, and F. Li, "Mixed-integer linear programming-based splitting strategies for power system islanding operation considering network connectivity," *IEEE Systems Journal*, vol. 12, no. 1, pp. 350–359, 2018.

[29] R. Menke, E. Abraham, P. Parpas, and I. Stoianov, "Approximation of system components for pump scheduling optimisation," *Procedia Engineering*, vol. 119, pp. 1059–1068, 2015.

[30] L. Rossman, W. H, M. Tryby, F. Shang, R. Janke, and T. Haxton, "Epanet 2.2 Users Manual, US Environmental protection agency," *EPA/600/R-20/133, Washington, DC*, 2020.

[31] G. D. Corporation, "General Algebraic Modeling System (GAMS) Release 35.2.0," Fairfax, VA, USA, 2021. [Online]. Available: http://www.gams.com/

[32] Cplex IBM ILOG, "V12. 1: User's manual for cplex," *International Business Machines Corporation*, vol. 46, no. 53, p. 157, 2009.